Observation of Single Photon Interference and Hong-Ou-Mandel Dip

P.Munkhbaatar[1,*] Ts.Baatarchuluun[2], D.Ulam-Orgikh[1], J.Davaasambuu[1], and K.Myung-Whun[3]

[1]*Department of Physics, National University of Mongolia, Ulaanbaatar 210646, Mongolia*

[2]*Department of Geology and Geophysics, National University of Mongolia,Ulaanbaatar 210646, Mongolia*

[3]*Department of Physics, Chonbuk National University, 561-756 Jeon-ju, Korea*

We have built a cost effective Hong-Ou-Mandel (HOM) interferometer by using a conventional cheap multimode laser and a home-made coincidence counting circuit and we have observed the single photon interference and HOM dip making us to measure the bandpass filter. We expect it could be a good model to the graduates trying a variety of quantum optics experiments.

PACS numbers: 78.47.J-, 78.66.Db

I. INTRODUCTION

Quantum mechanical approach on the modern optics leads to realize not only many new technologies such as Quantum communications, Quantum Computing and Quantum Imaging etc but also new experimental methods to solve fundamental questions in the entire physics. Many universities in the world have been trying to make a variety of simple and economic signal processing devices for researching quantum optics area not only because the price of its typical devices such as NIM processors supplied by ORTEC is quite expensive around USD$50,000 but also because it becomes necessary that the undergraduates should learn the quantum optics area.

Nevertheless, many researchers tend to be skeptical on those simple devices just because those are cheap. In this regards, we decided to make a low cost coincidence circuit designed by Dr. Kim Tae Hyun in 2005[1] and succeeded to realize two quantum optics experiments, single photon interference and Hong-Ou-Mandel(HOM) dip with it. The cost impact was significant that it was just USD$200 only. Spontaneous parametric down-conversion (also known as SPDC, or parametric scattering) is an important process in quantum optics, used especially as a source of entangled photon pairs, and of single photons. We succeeded in the generation of a entangled photons state using a multi mode 405 nm laser and its cost was only USD$50, which also made big cost impact in comparison to a typical single mode 405 nm laser whose price is around between USD$2,000 and 20,000.

We expect our setup to be one of the available models for the graduate students to try many quantum optics experiments in Korea and Mongolia. We used type-I beta-Barium Borate(-BBO) designed by 29.3^0 and 200 mW 405 nm multi-mode laser to generate spontaneous parametric down conversion light as a light source and tried two experiments, single photon interference and HOM dip.

II. CORRELATION FUCNTIONS OF SPDC

Figure 1 and 3 shows the proposed measurement setup. Here the photon pairs can be produced in pulsed mode by means of SPDC. A type-I nonlinear crystal is pumped by monochromatic and classical field with frequency ω_p. The pulsed photon pairs can be described by a nonseparable wave function $|\Psi\rangle$:

$$|\Psi\rangle = \int d\omega_s d\omega_i \mathrm{sinc}(\Delta L/2) e^{-i\Delta L/2} a_s^\dagger(\omega_s) a_i^\dagger(\omega_i)|0\rangle, \tag{1}$$

where $a_s^\dagger(\omega_s)(a_i^\dagger(\omega_i))$ is field creation operator for signal (idler) photon with $\omega_s(\omega_i)$ frequency, $\Delta = \mathbf{k}_p(\omega_p) - \mathbf{k}_s(\omega_s) - \mathbf{k}_i(\omega_i)$ and L is the thickness of nonlinear crystal. We ignored normalization constant for simplicity. Fock state $a_s^\dagger a_i^\dagger|0\rangle$ has one photon in each mode $\mathbf{k}_s$ and $\mathbf{k}_i$. Since the condition $\omega_s + \omega_i = \omega_p$ has to be satisfied at all times, we can simplify the above equation further by introducing the detuning frequency $\nu = \omega_s - \omega$ or equivalently, $\nu = \omega - \omega_i$ where $\omega = \omega_p/2$. We therefore obtain

$$|\Psi\rangle = \int_{-\infty}^{\infty} d\nu F(\nu) P(\nu) a_s^\dagger(\omega+\nu) a_i^\dagger(\omega-\nu)|0\rangle,$$

Where F is the joint spectral function for the signal and the idler photons that determines the coherence properties of state, and P is the frequency-dependent phase term. Note also that this expression clearly shows the frequency anticorrelated feature of the signal and the idler photons. For type I SPDC, the joint spectral function are the frequency-dependent phase term are given as:

$$F(\nu) = \mathrm{sinc}(\nu^2 D'' L/2), R(\nu) = exp(-i\nu^2 D'' L/2),$$

where the group-velocity dispersion (in the crystal) $D'' = d^2k/d\omega^2$. (Note $k_s = k_i$ for type I SPDC.) The first-order correlation function of the state can be calculated as following:

$$G^{(1)}(\tau) = \langle\Psi|E_s^{(-)}(t)E_s^{(+)}(t+\tau)|\Psi\rangle,$$

*Electronic address: p_munhkbaatar@yahoo.com

where $E_s^{(-)}(t) = \int_0^\infty d\omega a_s^\dagger(\omega)\exp(i\omega t)$ and $E_s^{(+)}(t) = \int_0^\infty d\omega a_s(\omega)\exp(-i\omega t)$. The first-order correlation function of the signal photon can then be calculated as

$$G^{(1)}(\tau) = \int_{-\infty}^{\infty} d\nu F(\nu)^2 \exp\left(-i\nu\tau\right).$$

As we can clearly see, the first-order correlation function of the signal photon is simply a Fourier transform of the power spectrum of the signal photon. The second-order correlation function can be calculated rather simply by using the state,

$$G^{(2)}(\tau) = |\langle 0|E_i^{(+)}(t)E_s^{(+)}(t+\tau)|\Psi\rangle|^2,$$

where $E_{i/s}^{(+)}(t) = \int_0^\infty d\omega a_{i/s}(\omega)\exp(-i\omega t)$. It is straightforward to obtain

$$G^{(2)}(\tau) = \left|\int_{-\infty}^{\infty} d\nu F(\nu)P(\nu)\exp(-i\nu\tau)\right|^2$$

Note that $G^{(1)}(\tau)$ and $G^{(2)}(\tau)$ can have quite deferent shape even though they are associated with the same $F(\nu)$. For example, $G^{(1)}(\tau)$ is not affected by the introduction of group-velocity dispersion between the source and detector, but $G^{(2)}(\tau)$ is broadened by it because any dispersion introduced in $E_s^{(-)}(t)$ simply cancels when calculating $G^{(1)}(\tau)$. In the case of $G^{(2)}(\tau)$, this cancellation does not happen because two different fields are involved[2].

III. ONE- AND TWO-PHOTON WAVE PACKETS

We have so far calculated first- and second-order correlation functions of the quantum state of SPDC. In this section, we study how these correlation function are actually linked to one-photon and two-photon wave packets in simple interference experiments.

For one-photon wave-packet measurement, we consider the output of a simple MachZehnder(MZ) interferometer, in which either the signal or the idler photons are the input. For the two-photon wave-packet measurement, we consider a well-known HOM interferometer setup, in which the signal-idler photon pair is made to interfere at a beam splitter, and the coincidence counts between single photon counter(SPC)s, which are placed at the output ports of the beam splitter, are measured.

Let us first calculate the SPC rate at the output port of a MZ interferometer shown in Fig.1 when the signal photon of SPDC is the input. In this case, the SPC rate is proportional to S,

$$S = \langle\Psi|E_A^{(-)}(t)E_A^{(+)}(t)|\Psi\rangle,$$

Where the $E_A^{(+)}(t) = \int_0^\infty d\omega\{a_s(\omega)\exp(-i\omega t) + a_s(\omega)\exp[-i\omega(t+\tau)]\}$ and τ is the delay between the two arm of the interferometer. It is then easy to show that

$$S = \int_{-\infty}^{\infty} d\nu F(\nu)^2\{1+\cos[(\nu+\omega)\tau]\},$$

which can be rewritten as

$$S \sim 1/2\{1+g^{(1)}(\tau)\cos(\omega\tau)\}, \qquad (2)$$

Where $g^{(1)}(\tau) = |G^{(1)}(\tau)|/|G^{(1)}(0)|$. Therefore the envelope of the interference fringe or the one photon wave packet observed at the output of the MZ interferometer directly corresponds to the first-order correlation function $G^{(1)}(\tau)$. Now we can calculate coincidence count:

$$C = \int |\langle 0|E_A^{(+)}(t_1)E_B^{(+)}(t_2)|\Psi\rangle|^2 dt_1 dt_2,$$

Where the $E_B^{(+)}(t) = \int_0^\infty d\omega a_i(\omega)\exp(-i\omega\tau)$. It is then easy to show that

$$C \sim \int_{-\infty}^{\infty} d\nu F(\nu)^2\{1+\cos[(\nu+\omega)\tau]\} = S. \qquad (3)$$

For a two-photon wave packet, we need to calculate the coincidence count rates for HOM interferometric setup shown in Fig.3. Consider the following setup: the signal and idler photons are generated at the crystal, propagate at different directions, reflect off at mirrors, and are made to interfere at a beam splitter. The both phonons have the same polarization, the delay between the two paths is τ. A detector package that consists of a single photon counters and a infrared bandpass filter is placed at each output port of the beam splitter, and the coincidence counts between the two detectors are recorded(see experimental setup shown in Fig. 3). The coincidence count rate is then proportional to C,

$$C = \int |\langle 0E_A^{(+)}(t_1)E_B^{(+)}(t_2)\Psi\rangle|^2 dt_1 dt_2.$$

The quantized electric fields $E_A^{(+)}(t_1)$ and $E_B^{(+)}(t_2)$ at the SPC-A and -B can be written as

$$
\begin{aligned}
E_A^{(+)}(t_1) &= \int_0^{\infty} d\omega \{a_s(\omega)\exp(-i\omega t_1) - i a_i(\omega)\exp[-i\omega(t_1+\tau)]\}, \\
E_B^{(+)}(t_2) &= \int_0^{\infty} d\omega \{-i a_s(\omega)\exp(-i\omega t_2) + a_i(\omega)\exp[-i\omega(t_2+\tau)]\},
\end{aligned}
$$

where τ is the delay introduced between the two arms of interferometer, t_1 and t_2 are the times at which the SPC-A and -B click, and the phase factor i comes from the reflection at the beam splitter. We get

$$
\begin{aligned}
C &= \int dt_+ dt_- \int d\nu d\nu' F(\nu)F(\nu')P(\nu)P^*(\nu')\exp[i(\nu-\nu')\tau]\sin(\nu t_-)\sin(\nu' t_-) \\
&\approx \int d\nu F(\nu)^2 - \int d\nu F(\nu)^2 P(\nu)^2 \exp(i2\nu\tau) \sim 1 - g^{(1)}(2\tau). \qquad (4)
\end{aligned}
$$

It is interesting to note that the two-photon wave packet does not contain the second-order correlation function $G^{(2)}(\tau)$. This result has interesting implications: (i) C has the same envelope as S except that the C envelope is half of the S envelope: (ii) any dispersion element introduced in a HOM interferometer cannot affect the shape of the interference envelope since $g^{(1)}(\tau)$ is not affected by group-velocity dispersion[2].

IV. EXPERIMENT

In this section, we describe two experiments that are designed to test the theory made in previous sections.

Let us first describe the one photon wave-packet measurement of type I SPDC. The experimental setup can be seen in Fig.1. A 5-mm-thick type I barium borate (BBO) crystal was pumped by a 405nm laser beam generating 801nm noncollinear SPDC photons. The residual pump beam was removed by a beam dumping. The delay between the two arms of the MZ interferometer was introduced by moving mirror with a picomotor driver. A 632nm guide laser and white light source were used to align this system. Alignment of the MZ interferometer shown in Fig.1 was achieved by merging a 632nm (not far from 805nm) HeNe laser with white light source3. A key feature of the method is the overlap of the downconversion with the alignment He-Ne laser in the near and far field. The splitting is provided by a cube beam splitter BS1 used at non-normal incidence. The deflecting and translating of the moving mirror and the fixed mirror, and the tilt of BS2 are then adjusted such that a single interference fringe is observed by the eyes on a viewing screen at one output port of the BS2. At this stage the interferometer will be aligned, but since the laser coherence length is long, the optical paths are unlikely to be balanced. The paths of the MZ interferometer are balanced using a spectrally broad emitter (white light source) instead of He-Ne laser. Using spectrometer, interference is only observable at the output port of the recombining beam splitter BS2 when the optical paths of the interferometer are balanced to within $\sim 30\mu$m. The balancing was achieved through manual adjustment of the moving mirror delay such that strongly modulated fringes were observed by the eyes on a viewing screen of spectrometer.

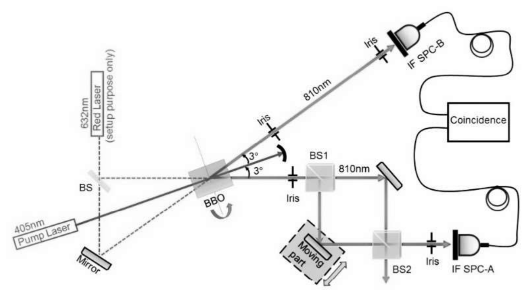

FIG. 1: Schematic of alignment interferometer and Mach-Zehnder interferometer. The red lines denote spontaneous parametric downconversion lights. The broken lines represent 632nm red laser which is for guide and alignment. IF is infrared filter. SPC is single photon count. BS is beam splitter

Photons were finally detected with detector packages that consist of a SPCs module. The distance from the BBO crystal to the detector was approximately 80cm, and all apertures used in this experiment were 3mm in diameter. For this measurement, we used a 10nm FWHM filter to suppress the pump light contamination that round $\tau = 0$.

Figure 2 shows the experimental data which is moving distance dependence single counts and coincidence count. Red and Green lines show SPC-A and -B, respectively. As discussed above, SPC-A is single photon interference. Black line shows coincidence count which is same envelop with SPC-A. Let

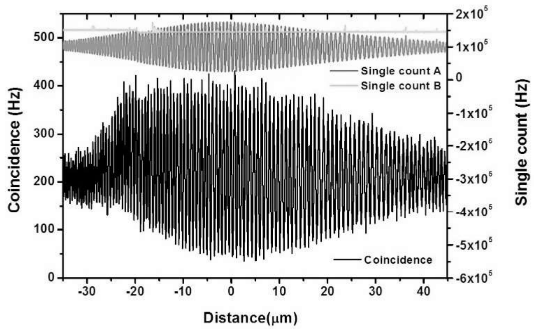

FIG. 2: Single photon interference experimental data. This figure is arm length dependence of coincidence and single counts.

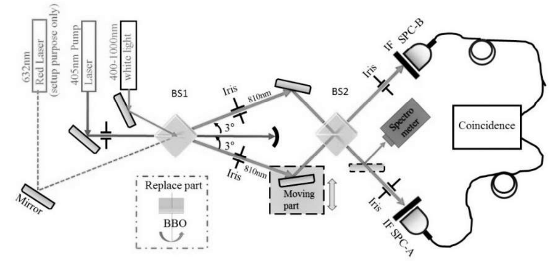

FIG. 3: Schematic of alignment/balancing interferometer and HOM interferometer. The components to the left of the apertures drawn with dashed red and green lines denote sources/optics for the interferometer alignment/balancing. The blue line denote pump light for SPDC. The solid red lines represent the common optical paths shared by the visible/HOM interferometers. The coincidence counter records the coincident detection events between the SPCs. FM is a flipper mirror. BS is beam splitter.

us now discuss the measurement of two-photon wave packets. To measure the two-photon wave packet, we should construct HOM interferometer. Two major requirements in the construction of the HOM interferometer are the alignment and length balancing of two optical paths. A method shown in ref[3] is used for meeting these requirements that requires no custom optics or expensive equipment. Using this method, a two photon interferometer sourced by degenerate noncollinear parametric photon pairs was aligned and the optical paths were balanced to within an average of 10μm, yielding two-photon interference features with visibilities of $\sim$ 0.9. The method is applicable to arbitrary noncollinear emission angles, including nondegenerate downconversion situations where the signal and idler emission angles differ.

Alignment was achieved by merging the framework of the HOM interferometer with a MZ interferometer illuminated by a 632nm (not far from 805nm) HeNe laser. Schematic layout is shown in Fig.3. The splitting is provided by a cube beam splitter BS1 used at non-normal incidence, in place of the nonlinear crystal. A key feature of the method is that aperture pairs are positioned for collection of the 805nm downconversion and define the trajectories in both the HOM and MZ interferometers. The aperture positioning is achieved by maximizing the count rate on single photon detectors placed along the emission direction. The signal to the detector should be band pass limited and centered at the desired wavelength. In order for the laser light to be guided through the HOM apertures, thus ensuring overlap of the downconversion with the alignment beams in the near and far field, the freedom to rotate and translate the beam splitter BS1 in the plane of the optical bench was necessary, in addition to directional control of the beam through mirror in output 632nm laser. The deflecting and translating of the moving mirror, and the tilt of BS2 are then adjusted such that a single interference fringe is observed by the eyes on a viewing screen at one output port of the second beam splitter. At this stage the interferometer will be aligned, but since the laser coherence length is long, the optical paths are unlikely to be balanced. The paths of the interferometer are instead balanced using the MZ framework, exchanging the laser for a spectrally broad emitter (white light) in another input of beam splitter BS1 by using a mirror. Using spectrometer, interference is only observable at the output port of the recombining beam splitter BS2 when the optical paths of the interferometer are balanced to within $\sim$ 10μm. The balancing was achieved through manual adjustment of the moving mirror delay such that strongly modulated fringes were observed by the eyes on a viewing screen of spectrometer.

Maximization of the detected singles counts from the guide laser through the interferometer enables the SPC positions to be tuned. Finally, the nonlinear crystal is repositioned in place of BS1 and the pump laser is applied. The phase match angle was fine tuned for maximum counts at the SPCs. Although the emission lines of the pump laser do not coincide with the band of the filters in front of SPCs, there was sufficient optical noise at the filter wavelengths for a singles count of $\sim 10^6 s^{-1}$. After alignment HOM interferometer, for HOM dip, visibilities of 0.60 shown in Fig.4 were measured by coincidence count when interferometer arm length is varied by the moving mirror in shown Fig.3. Accidental coincidences are subtracted from the raw data, which is simply calculated from the equation. $N_{acc} = \tau_r N_A N_B$, where N_A and N_B the single photon counting rates are 135kHz and 125kHz, respectively, and τ_r is coincidence resolution time, 6 ns in our experiment. The gray line in Fig. 4 corresponds to the

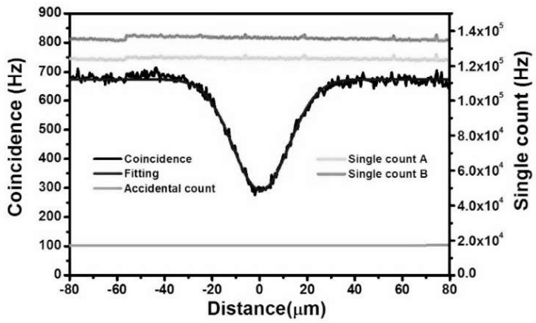

FIG. 4: HongOuMandel dip: HOM interferometer coincidence data are shown by black line. The blue line fit to the data is derived from Gaussian function HOM dip defined by the Fourier transform of the spectral filters. The green and red lines are single count A and B, respectively.

accidental counts.

V. RESULT AND DISCUSSION

First, we observed single photon interference, fringe changing recorded by coincidence and single counts with each moving part position. Single and coincidence counts were correlated or they have same envelopes. Although the sum frequency ${}_s + {}_i$ is very well defined in the experiment, the individual downshifted frequencies ${}_s$, ${}_i$ have large uncertainties, that, in practice, are largely determined by the bandpass infrared filter IF inserted in front of SPCs, as shown in Fig. 1 and 2. The envelope is defined by the filter band width instead of the $F(\nu)$ joint distribution function. Because band width of IF is smaller than that of the joint distribution function. Second, to make HOM experiment, we built a MZ type interferometer. Using white light source and spectral interference we made accurate alignment of HOM interferometer [3]. As previously mentioned, the Eq.(4) or the coincidence of HOM interferometer can be calculated by using the filter band distribution with Gaussian function width instead of the $F(\nu)$ joint distribution function. The first order correlation function has a Gaussian form[4]. After subtracting accidental counts, HOM interference is fitted by following equation:

$$N_c = c(T^2 + R^2)\left(1 - \frac{2RT}{T^2 + R^2} V e^{-x^2/\sigma^2}\right), \quad (5)$$

where V is visibility of HOM interference fringe, R and T are the reflectivity and transmissivity of the beam splitter with $R + T = 1$ ($T : R = 55 : 45$ splitting of BS2), c is another constant. From a fit to the data, we estimated the visibility to be $70 \pm 2\%$ and σ as 23μm. It is likely that most of the lost visibility may be attributed to wavefront distortion, the type I crystal due to complicated phase matching and misalignment of the interferometer due to human error[3]. By looking at the visibility, you can determine how pure your states are. We have observed around 70% visibility HOM dip, which made us possible to find the bandwidth range of interference filter used in this experiment which was 810 ± 12nm that made good agreement with manufacturing specification, 810 ± 10nm. In here, we present the results of two quantum optics, i.e. single photon interference and the HOM dip obtained from a cost-effective measurement system. We built a low cost coincidence circuit based on the design of a literature [1] and used a cheap (USD$50) conventional multi-mode laser as the light source. We observed different frequencies of coincidence and single count. We expected that is due to mismatch of center frequencies of band pass filter and down converted light.

VI. CONCULTION

By using recent advances in the production and detection of correlated photons, we developed a sequence of two experiments for graduates to demonstrate important aspects of quantum superposition. Doing these experiments will prepare students to understand issues of quantum cryptography, quantum computing, and quantum teleportation. More directly, the experiments will show that the photon exists, that a photon interferes with itself, that small modifications of the observing apparatus can erase and restore interference, and that there exist other kinds of photon interference than the one-photon sort. The apparatus will also be used to exhibit the nonlocal nature of quantum mechanics by showing the violation of Bells inequalities. Further, we will develop several important applications in the field of quantum information, for example, quantum teleportation, quantum repeater, linear optics quantum computation, and quantum optical coherence tomography, among others.

Acknowledgments

This research was supported by the National Research Foundation of Mongolia (Grant No. SSA 017/2016).

[1] T. Kim et al, Low-cost nanosecond electronic coincidence detector, arXiv:Physics/0501141v1
[2] Yoon-Ho Kim, Measurement of one-photon and two-photon wave packets in spontaneous parametric downconversion, J. Opt. Soc. Am. B **20**, 1959(2003)
[3] P. J. Thomas et al, The Hong-Ou-Mandel interferometer: A new procedure for alignment, Review of Scientific Instrument **80**, 036101(2009)
[4] C. K. Hong et al, Measurement of subpicosecond time intervals between two photons by interference, Phys. Rev. Lett. **59**, 2044(1987)